



Two Novel Single-Chain Variable Fragments, EB211 and EB279, Exert Antibacterial Activity Against *Acinetobacter baumannii* by Destabilizing the Outer Membrane

Eilnaz Basardeh¹, Farzaneh Nazari¹, Abolfazl Fateh¹, Seyed Davar Siadat¹, Akbar Oghalaie², Masoumeh Azizi³, Fatemeh Rahimi-Jammani^{1*}

¹Department of Mycobacteriology and Pulmonary Research, Microbiology Research Center, Pasteur Institute of Iran, Tehran, Iran; ²Department of Medical Biotechnology, Biotechnology Research Center, Pasteur Institute of Iran, Tehran, Iran; ³Molecular Medicine Department, Biotechnology Research Center, Pasteur Institute of Iran, Tehran, Iran

ARTICLE INFO

Original Article

Keywords: *Acinetobacter baumannii*, Antibacterial agents, Monoclonal antibodies, Single-chain variable fragments, Magnesium

Received: 19 Aug. 2024

Received in revised form: 30 Nov. 2024

Accepted: 09 Dec. 2024

DOI: 10.61186/JoMMID.12.4.299

*Correspondence

Email: Rahimi@pasteur.ac.ir;

Redogunerahimi@gmail.com

Tel: +982166953311

Fax: +982166465132

© The Author(s)



ABSTRACT

Introduction: *Acinetobacter baumannii* is notorious for its high resistance levels, and the development of clinically effective antimicrobial agents is an urgent medical challenge. Single-chain variable fragments (scFvs) that exhibit antibacterial properties against challenging pathogens, such as *Pseudomonas aeruginosa* and *Staphylococcus aureus*, have the potential to improve therapeutic strategies significantly. Their unique ability to function independently of the host immune system makes scFvs a highly promising option for effective treatment. In our previous studies, we identified two human scFvs (EB211 and EB279) that showed direct growth inhibition activity against *A. baumannii* strains *in vitro* and therapeutic effectiveness in immunocompromised mice with pneumonia caused by an extensively drug-resistant *A. baumannii* strain. In the present study, we endeavored to demonstrate how EB211 and EB279 could inhibit the growth of *A. baumannii*. **Methods:** *A. baumannii*, *Klebsiella pneumoniae*, and *Pseudomonas aeruginosa* strains were individually incubated with the scFv in the presence of a high concentration of magnesium (MgSO₄; 20 mM). Epitope mapping and immunoblotting were conducted to identify *A. baumannii* proteins likely bound by EB211 and EB279. **Results:** It was found that EB211 and EB279, similar to colistin sulfate, lost their activity in the presence of magnesium. Moreover, immunoblotting revealed that EB211 and EB279 might bind the OprD family outer membrane porin and TonB family C-terminal domain protein, respectively. **Conclusion:** EB211 and EB279 elicit direct growth inhibitory activity against *A. baumannii* without needing immune cells or complements, which could be helpful for immunocompromised patients.

INTRODUCTION

Acinetobacter baumannii is an opportunistic pathogen that causes deadly infections in hospitals and the community [1]. It is one of the most problematic nosocomial ESKAPE pathogens due to its resistance to last-resort antibiotics (e.g. colistin and tigecycline) [1]. Accordingly, the World Health Organization (WHO) has advocated the development of effective antimicrobial agents against carbapenem-resistant *A. baumannii* (CRAB) [2]. The development of functional antibacterial agents has been facilitated by demonstrating that cationic antibacterial agents (e.g. antimicrobial peptides and positively charged antibodies) can exert effective growth

inhibitory activity through electrostatic interactions with the outer membrane or cell wall of bacteria [3-5]. Of note, *A. baumannii* benefits from virulence factors such as outer membrane proteins (OMPs), metal ion acquisition systems, lipopolysaccharides (LPS), and efflux pumps, empowering it to survive harsh environments (e.g. host immune system and hospital environments) and resist antibiotics [6-10]. Several studies have demonstrated that mAbs targeting these virulence factors could protect against infections caused by multidrug-resistant (MDR) or extensively drug-resistant (XDR) *A. baumannii* in animal models [6, 11-14].

Antibody fragments with growth inhibitory activity are an emerging class of antibacterial agents exhibiting significant inhibitory activity against some health-threatening pathogens (e.g. *Acinetobacter baumannii*, *Staphylococcus aureus*, and *Pseudomonas aeruginosa*) [1, 4, 15-18]. The single-chain variable fragment (scFv) consists of the variable domains of light and heavy chains (VL and VH, respectively) of a monoclonal antibody (mAb) connected by a peptide linker [19]. This antibody fragment, lacking the antibody constant domains, exerts its antibacterial activity through mechanisms including disrupting the outer membrane/cell wall of bacteria (functioning as antimicrobial peptides), interfering with the biological activity of vital macromolecules, acting as an abzyme, or causing apoptosis [1, 4, 16, 17, 20]. In this regard, Richard et al. showed that the S20 scFv caused cell damage and death by targeting the O-specific antigen of *P. aeruginosa* (serotype O6) [15]. Moreover, Soltanmohammadi et al. indicated that three human scFvs by binding to vital *S. aureus* proteins, including TrkH family potassium uptake protein, peptidoglycan editing factor (PgeF), and lipoprotein-like 8 (lpl8), and disrupting the integrity of the cell wall led to bacterial death [4].

In previous studies, we found two human scFvs, EB211 and EB279, with significant growth inhibitory activity against *A. baumannii* *in vitro* [1] and *in vivo* [18]. In the present study, *A. baumannii* strains were incubated with the scFv (EB211 or EB279) and a high concentration of magnesium (Mg^{2+}) to demonstrate that these scFvs act as cationic antimicrobial peptides (cAMPs). Furthermore, we conducted epitope mapping and immunoblotting to determine which *A. baumannii* proteins might be targeted by EB211 and EB279.

MATERIALS AND METHODS

Bacterial strains and susceptibility testing. Two XDR strains of *A. baumannii*, A.b.56 and A.b.58 (from an endotracheal tube and the blood of two patients with *A. baumannii* infection, respectively) were obtained from the Microbiology Department of the Pasteur Institute of Iran [1, 21]. Methicillin-resistant *S. aureus* (MRSA) S.a.124 (from the blood of a patient with *S. aureus* infection) was obtained from the Department of Mycobacteriology and Pulmonary Researches of the Pasteur Institute of Iran [4]. *A. baumannii* ATCC 19606, *Klebsiella pneumoniae* ATCC 700603, and *P. aeruginosa* ATCC 27853 were from the American Type Culture Collection. The strains were routinely cultured on trypticase soy broth (TSB; Sigma-Aldrich, Saint Louis, USA) or trypticase soy agar (TSA; Sigma-Aldrich).

Determination of the potential of EB211 and EB279 as cationic antimicrobials. *Acinetobacter baumannii* ATCC 19606, *A. baumannii* A.b.56, *A. baumannii* A.b.58, *K. pneumoniae* ATCC 700603, and *P.*

aeruginosa ATCC 27853 have previously been evaluated for antimicrobial susceptibility [1]. It was determined that *A. baumannii* ATCC 19606, *A. baumannii* A.b.56, *A. baumannii* A.b.58, and *P. aeruginosa* ATCC 27853 were colistin-susceptible strains with a minimum inhibitory concentration (MIC) of 1 $\mu\text{g}/\text{mL}$ based on the MIC breakpoints of the Clinical and Laboratory Standards Institute (CLSI) for colistin sulfate (CS). Additionally, *K. pneumoniae* ATCC 700603 was susceptible to imipenem, with a MIC of 2 $\mu\text{g}/\text{mL}$ [1].

One of the assays that can exhibit the antibacterial agent's impact on the integrity of the bacterium's outer membrane is to culture in a high concentration of Mg^{+2} [4]. To this end, the antibacterial activity of EB211 and EB279 against *A. baumannii* ATCC 19606, A.b.56, and A.b.58, *K. pneumoniae* ATCC 700603, and *P. aeruginosa* ATCC 27853 was investigated in the presence of a high concentration of $MgSO_4$ by microtiter and agar plate assays as previously described [4]. In brief, the growth curves of bacteria incubated with the scFv (200 $\mu\text{g}/\text{mL}$) [1] or the antibiotic (CS; 1 $\mu\text{g}/\text{mL}$ or imipenem; 0.125 $\mu\text{g}/\text{mL}$) [1] in the presence of $MgSO_4$ (20 mM) (Merck, Darmstadt, Germany) [4] were compared with the growth curves of bacteria incubated with the scFv or the antibiotic in the absence of $MgSO_4$ (microtiter plate assay) [1]. Furthermore, the viability of bacteria incubated with the scFv or the antibiotic (CS or imipenem) in the presence of $MgSO_4$ was determined after 30 minutes and five hours of incubation by plating the mixture on LB agar (or LB agar containing imipenem) and counting the colonies after 18 hours of incubation at 37°C (agar plate assay) [1].

Prediction of EB211- and EB279-specific target proteins. The Ph.D.TM-C7C Phage Display Peptide Library (~ 10⁹ clones) (New England Biolabs, Beverly, MA, USA) was biopanned against EB211 and EB279 to isolate phage clones specific to the scFv (EB211 or EB279), according to the Ph.D.-C7C kit instructions. Phage DNAs were extracted from four phage clones, infected with eluted phages from the third round of panning on each scFv, according to Ph.D.-C7C kit instructions. After sequencing, the nucleotide sequence of peptides was analyzed by the Gene Runner program, version 6.0 (Hastings Software, Inc.). The amino acid sequences of the inserts were appraised in the Biopanning Data Bank (MimoDB) (<http://immunet.cn/bdb/>), and the peptides unrelated to the target were erased [22, 23]. Then, the peptides were blasted against the NCBI protein database for *A. baumannii*, and proteins with a score ≥ 18.5 were predicated as proteins targeted by EB211 or EB279 [4].

Immunoblotting. Total-cell envelopes of *A. baumannii* A.b.56 were prepared as previously described [24]. Briefly, an overnight culture of *A. baumannii* A.b.56 was centrifuged at 8000 g for 10 min. The pellet was homogenized in 1.5 mL of 10 mM Tris-HCl-0.3%

NaCl pH 8.0, followed by sonication. The suspension was centrifuged, and the supernatant was transferred into a new microtube, followed by centrifugation for 60 min at 20,000g.

Total-cell envelopes of *A. baumannii* A.b.56 and the cell wall extract of *S. aureus* S.a. 124 [4] were separated by sodium dodecyl sulfate-polyacrylamide gel electrophoresis (SDS-PAGE), followed by immunoblotting. In brief, the polyvinylidene fluoride (PVDF) membranes were individually incubated with EB211 and EB279 (800 µg/mL), followed by the incubation with mouse anti-human scFv polyclonal antibody (1:200 dilution). After incubation with goat anti-mouse IgG-horseradish peroxidase (HRP)-conjugated antibody (1:2000 dilution), the membranes were developed with 3,3'-Diaminobenzidine (DAB)/H₂O₂.

Statistical analysis. All results are presented as the mean ± standard error of the mean (SEM) of data from at least three independent experiments. Statistical significance was determined using one-way analysis of variance (ANOVA), followed by Dunnett's multiple-comparison test. The differences were considered statistically significant at $P < 0.05$. GraphPad Prism version 8 software (<https://www.graphpad.com/>) was used for all analyses.

Ethical considerations. In this study, bacterial strains and *in vitro* assays did not involve human or animal subjects, so approval from an ethics committee was not required. All procedures were conducted in accordance with institutional guidelines for laboratory research.

RESULTS

The potential of EB211 and EB279 as cationic antimicrobials. We hypothesized that the EB211 and EB279 scFvs exert their antibacterial activity as cAMPs by interacting with negatively-charged LPS in the outer membranes of Gram-negative bacteria, leading to destabilization and permeabilization of the membrane [3-5, 25]. To this end, the amino acid sequence of both scFvs was assessed in the ProtParam tool on the ExPASy bioinformatics website. It has been shown that EB211 and EB279 have an isoelectric point (pI) of 9.37 and 9.14, respectively, due to the presence of positively charged residues (arginine and lysine) [1]. The negative grand average of hydropathicity (GRAVY) values showed that none of the complementarity-determining regions (CDRs) had a hydrophobic nature. The CDRs of EB211 and EB279 were also assessed in the Antimicrobial Peptide Database (APD), and no matches were identified. However, the addition of MgSO₄ (20 mM) could completely inhibit the antibacterial activity of EB211, EB279, and CS against *A. baumannii* ATCC 19606, A.b.56, A.b.58, and *P. aeruginosa* ATCC 27853

(Figures 1-4). Moreover, although EB211 and EB279 lost their growth inhibitory activity against *K. pneumoniae* ATCC 700603, imipenem maintained its antibacterial effect in the presence of a high concentration of Mg⁺² (Figure 5).

Targeting *A. baumannii* proteins with EB211 and EB279. To investigate whether EB211 and EB279 also interact with *A. baumannii* envelope proteins, a peptide-expressing phage display library (Ph.D.TM-C7C Phage Display Peptide Library) was enriched against these scFvs. The enrichment led to the isolation of eight phage clones. After sequencing, among four phage clones related to EB211, two clones showed a mutual sequence (-CLRSPDRSC-; 50%), and the rest encoded a peptide sequence (-CIQSPRHTC-; 50%). All four clones related to EB279 presented a peptide sequence (-CTNIPVGTC-; 100%). Three peptide sequences were analyzed in the MIMO database, and the data demonstrated that all peptides were true target binders. Next, the sequences were subjected to a BLASTp against the NCBI protein database for *A. baumannii*. The proteins that scored above 18 were selected for further evaluation in the UniProt database. Among the proteins identified as having the EB211-specific peptide, -CIQSPRHTC-, were ATP-binding cassette (ABC) transporters, the efflux resistance-nodulation-division (RND) transporter permease subunit, and the type IV pilin protein. A second EB211-specific peptide, -CLRSPDRSC-, was also found in proteins such as ABC transporters, the OprD family outer membrane porin, and the mechanosensitive ion channel family protein.

Last but not least, the penicillin-binding protein (PonA), the major facilitator superfamily (MFS) permease, the TonB family C-terminal domain protein, the type IV pilus modification protein PilV, and the RND type efflux pump were among the proteins with the highest scores, anticipated from blasting the peptide related to EB279 (-CTNIPVGTC-) and considered to be the target proteins of EB279.

To determine the candidate *A. baumannii* proteins, the reactions of EB211 and EB279 with the total membrane extract of *A. baumannii* A.b.56 and the cell wall extract of *S. aureus* S.a.124 were assessed by SDS-PAGE and immunoblotting (Figure 6A and B).

As illustrated in Figure 6B, EB211 detected a sharp band around 50 kDa, close to the molecular weight of the OprD family outer membrane porin (49.1 kDa) predicted from the EB211-specific peptide (-CLRSPDRSC-). Furthermore, EB279 identified a single band around 25 kDa, close to the molecular weight of the TonB family protein (TonB family C-terminal domain) (24.4 kDa) predicted from the EB279-specific peptide (-CTNIPVGTC-) (Figure 6B).

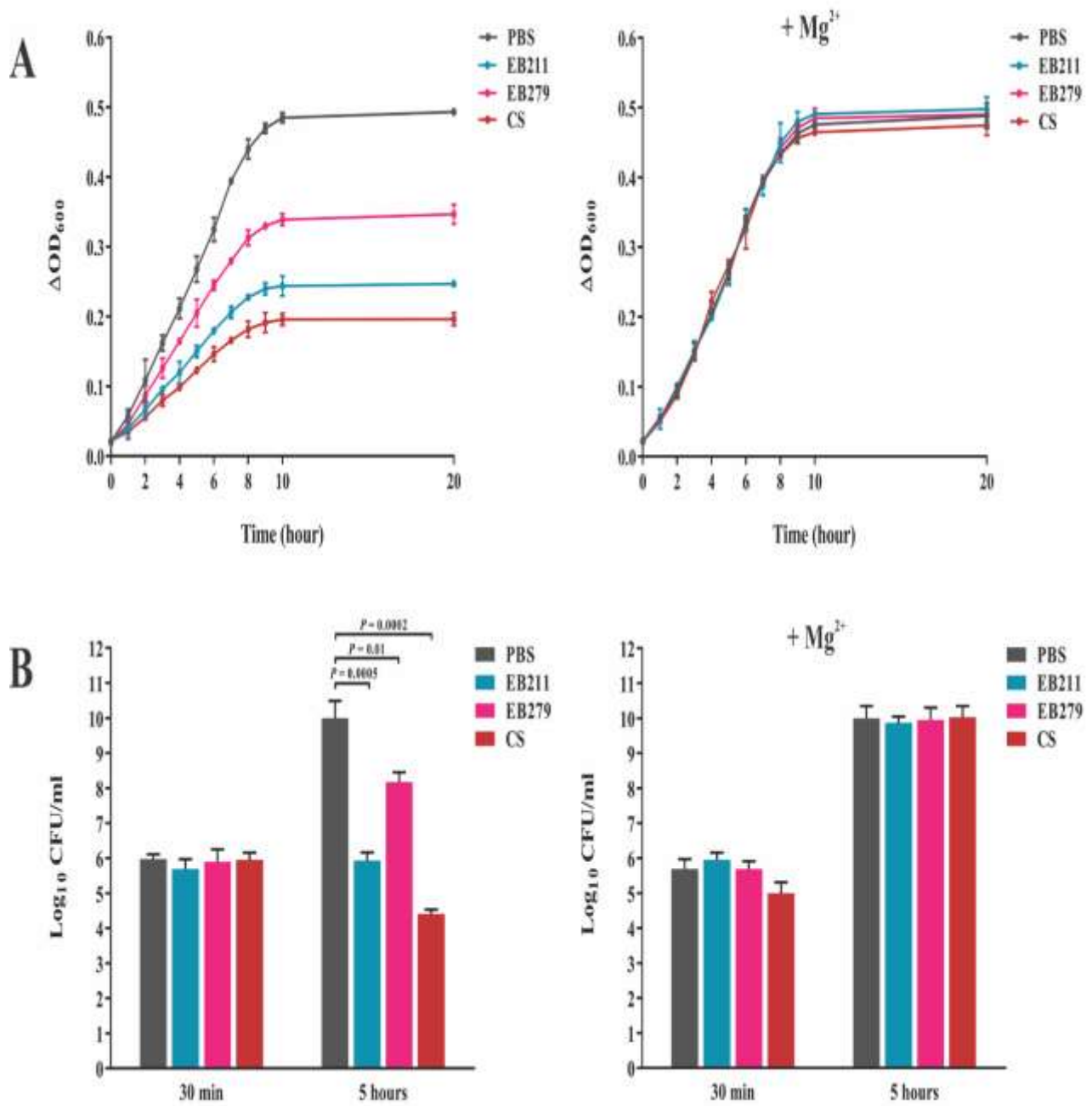


Fig. 1. Antibacterial activity of EB211 and EB279 against *A. baumannii* ATCC 19606 was nullified in the presence of a high concentration of Mg^{2+} . **(A)** Microtiter plate assay. *A. baumannii* ATCC 19606 ($OD_{600} \approx 0.02$) was incubated with EB211 (200 $\mu\text{g/mL}$), EB279 (200 $\mu\text{g/mL}$), colistin sulfate (CS) (1 $\mu\text{g/mL}$), or phosphate-buffered saline (PBS) in the absence or presence of 20 mM $MgSO_4$ for 20 hours. The growth was monitored by reading the optical density at 600 nm every hour for 10 hours and after 20 hours. The effect of EB211, EB279, and CS on the growth curve of *A. baumannii* ATCC 19606 disappeared in the presence of 20 mM $MgSO_4$. **(B)** Agar plate assay. *A. baumannii* ATCC 19606 ($OD_{600} \approx 0.02$) was incubated with EB211 (200 $\mu\text{g/mL}$), EB279 (200 $\mu\text{g/mL}$), CS (1 $\mu\text{g/mL}$), or PBS in the absence or presence of 20 mM $MgSO_4$ for five hours. At 30 min and five hours of incubation, the mixtures were plated on LB agar, followed by the enumeration of colonies grown after 18 hours of incubation at 37°C. At a high concentration of Mg^{2+} , EB211, EB279, and CS were ineffective against *A. baumannii* ATCC 19606. The results represent the mean \pm standard error of the mean (SEM) of three independent experiments run in triplicate. Statistical significance was determined by one-way analysis of variance (ANOVA) for each time point, followed by Dunnett's multiple-comparison test against the PBS control group.

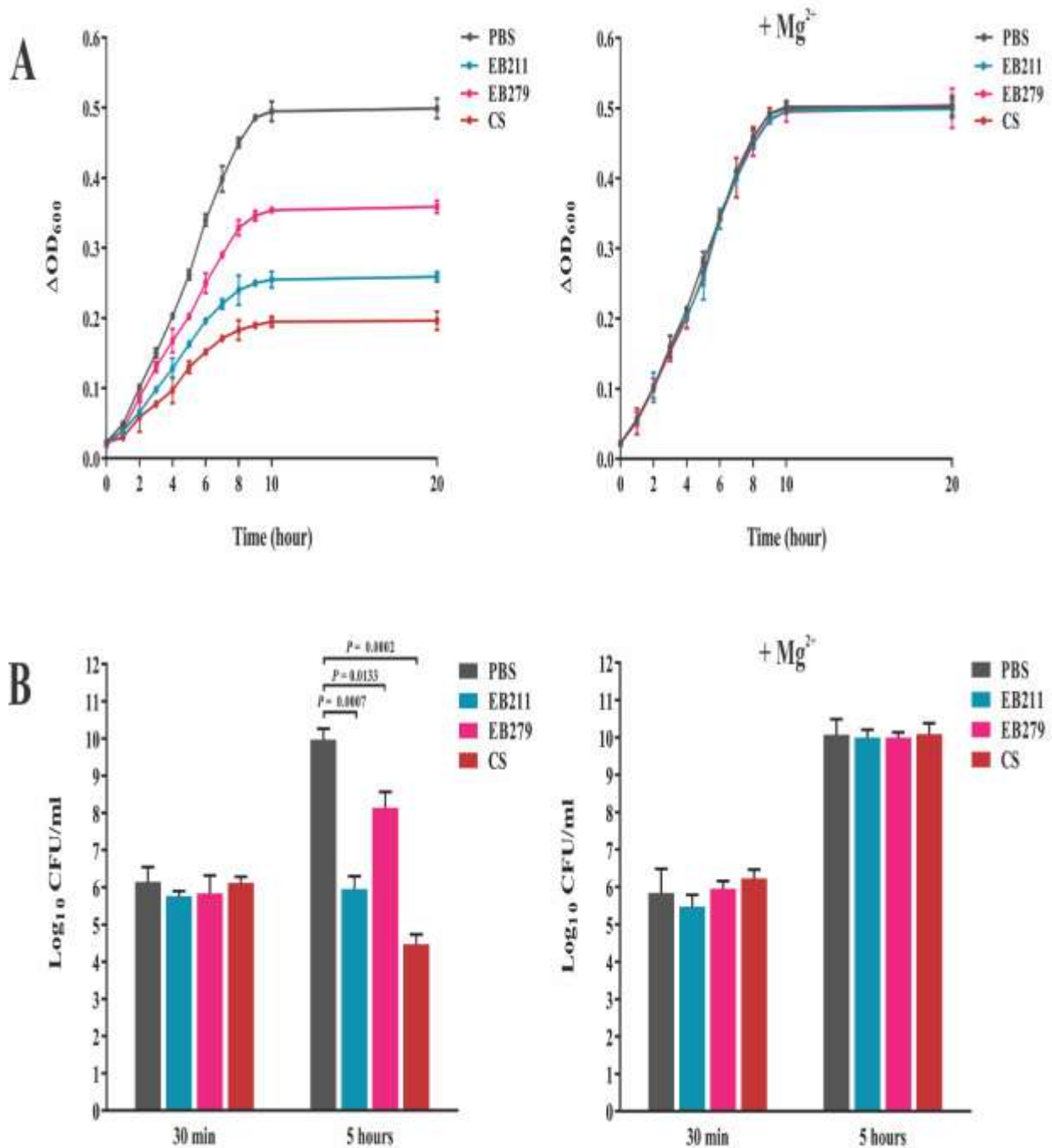


Fig. 2 Antibacterial activity of EB211 and EB279 against *A. baumannii* A.b.56 was abrogated in the presence of a high concentration of Mg^{2+} . **(A)** Microtiter plate assay. *A. baumannii* A.b.56 ($OD_{600} \approx 0.02$) was incubated with EB211 (200 $\mu\text{g}/\text{mL}$), EB279 (200 $\mu\text{g}/\text{mL}$), colistin sulfate (CS) (1 $\mu\text{g}/\text{mL}$), or phosphate-buffered saline (PBS) in the absence or presence of 20 mM $MgSO_4$ for 20 hours. The growth was monitored by reading the optical density at 600 nm every hour for 10 hours and after 20 hours. The effect of EB211, EB279, and CS on the growth curve of *A. baumannii* A.b.56 disappeared in the presence of 20 mM $MgSO_4$. **(B)** Agar plate assay. *A. baumannii* A.b.56 ($OD_{600} \approx 0.02$) was incubated with EB211 (200 $\mu\text{g}/\text{mL}$), EB279 (200 $\mu\text{g}/\text{mL}$), CS (1 $\mu\text{g}/\text{mL}$), or PBS in the absence or presence of 20 mM $MgSO_4$ for five hours. At 30 min and five hours of incubation, the mixtures were plated on LB agar supplemented with imipenem, followed by the enumeration of colonies grown after 18 hours of incubation at 37°C. At a high concentration of Mg^{2+} , EB211, EB279, and CS were ineffective against *A. baumannii* A.b.56. The results represent the mean \pm standard error of the mean (SEM) of three independent experiments run in triplicate. Statistical significance was determined by one-way analysis of variance (ANOVA) for each time point, followed by Dunnett's multiple-comparison test against the PBS control group.

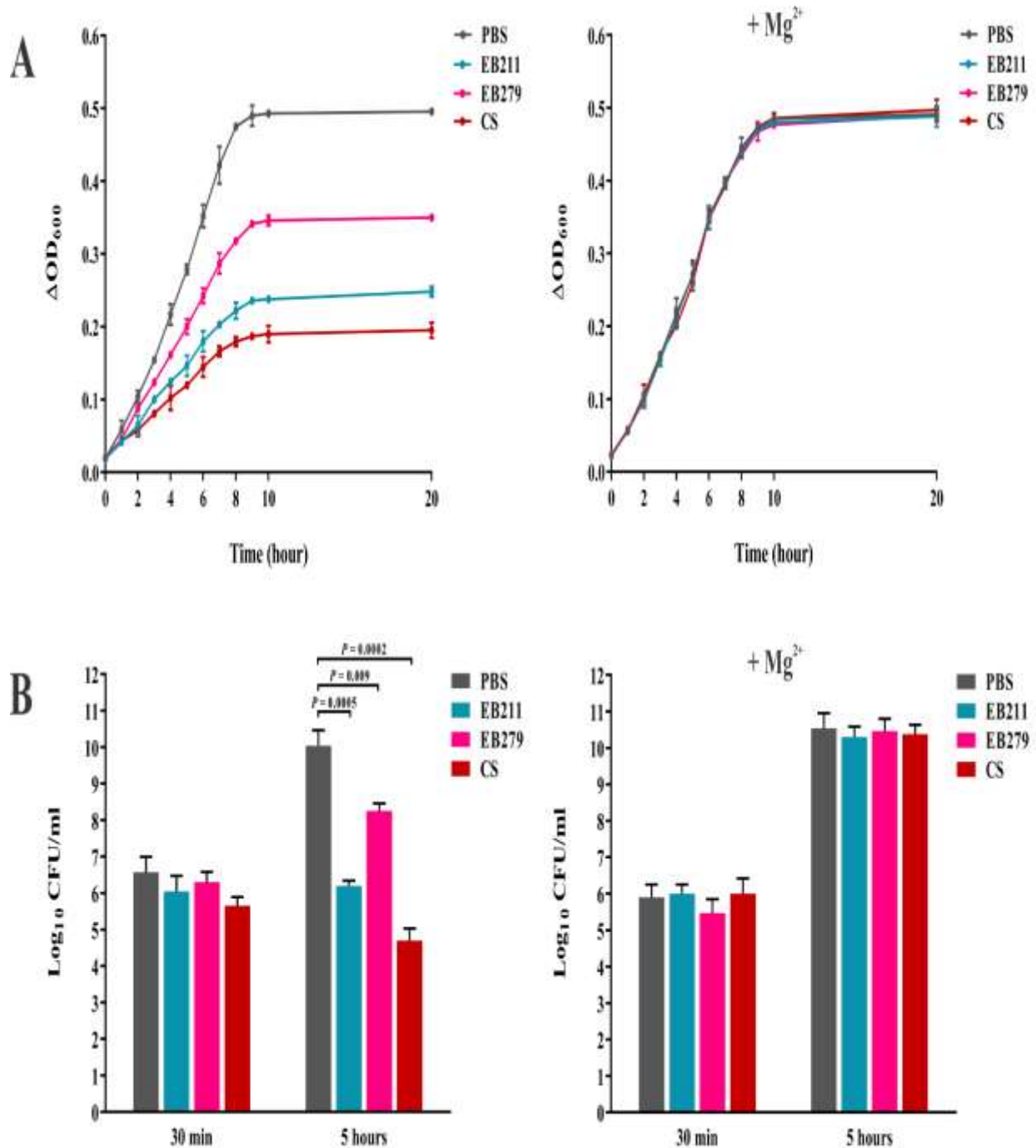


Fig. 3 Antibacterial activity of EB211 and EB279 against *A. baumannii* A.b.58 was negated in the presence of a high concentration of Mg^{2+} . (A) Microtiter plate assay. *A. baumannii* A.b.58 ($OD_{600} \approx 0.02$) was incubated with EB211 (200 $\mu\text{g/mL}$), EB279 (200 $\mu\text{g/mL}$), colistin sulfate (CS) (1 $\mu\text{g/mL}$), or phosphate-buffered saline (PBS) in the absence or presence of 20 mM $MgSO_4$ for 20 hours. The growth was monitored by reading the optical density at 600 nm every hour for 10 hours and after 20 hours. The effect of EB211, EB279, and CS on the growth curve of *A. baumannii* A.b.58 disappeared in the presence of 20 mM $MgSO_4$. (B) Agar plate assay. *A. baumannii* A.b.58 ($OD_{600} \approx 0.02$) was incubated with EB211 (200 $\mu\text{g/mL}$), EB279 (200 $\mu\text{g/mL}$), CS (1 $\mu\text{g/mL}$), or PBS in the absence or presence of 20 mM $MgSO_4$ for five hours. At 30 min and five hours of incubation, the mixtures were plated on LB agar supplemented with imipenem, followed by the enumeration of colonies grown after 18 hours of incubation at 37°C. At a high concentration of Mg^{2+} , EB211, EB279, and CS were ineffective *A. baumannii* A.b.58. The results represent the mean \pm standard error of the mean (SEM) of three independent experiments run in triplicate. Statistical significance was determined by one-way analysis of variance (ANOVA) for each time point, followed by Dunnett's multiple-comparison test against the PBS control group.

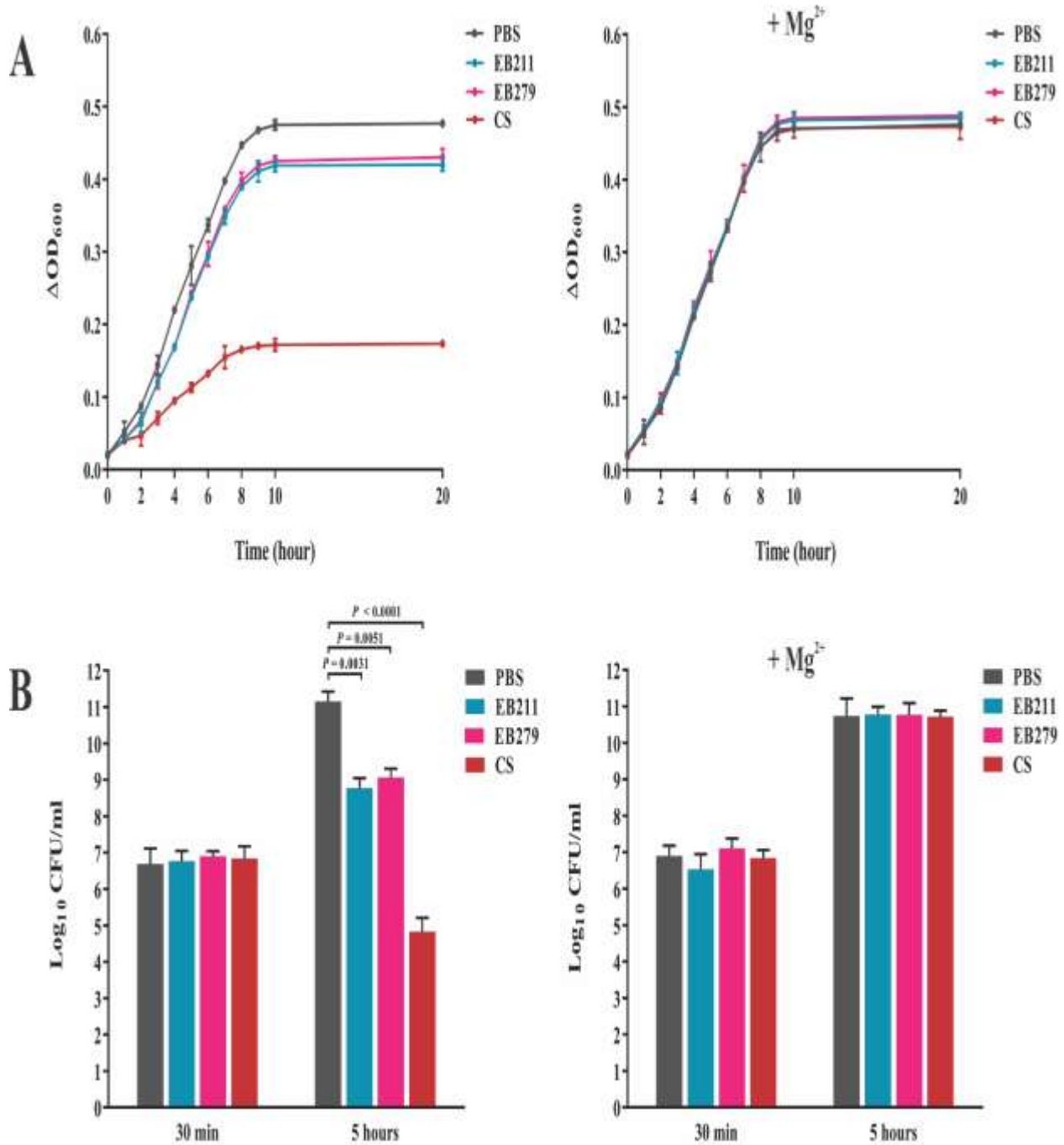


Fig. 4 Antibacterial activity of EB211 and EB279 against *P. aeruginosa* ATCC 27853 was nullified in the presence of a high concentration of Mg²⁺. (A) Microtiter plate assay. *P. aeruginosa* ATCC 27853 (OD₆₀₀ ≈ 0.02) was incubated with EB211 (200 μg/mL), EB279 (200 μg/mL), colistin sulfate (CS) (1 μg/mL), or phosphate-buffered saline (PBS) in the absence or presence of 20 mM MgSO₄ for 20 hours. The growth was monitored by reading the optical density at 600 nm every hour for 10 hours and after 20 hours. The effect of EB211, EB279, and CS on the growth curve of *P. aeruginosa* ATCC 27853 disappeared in the presence of 20 mM MgSO₄. (B) Agar plate assay. *P. aeruginosa* ATCC 27853 (OD₆₀₀ ≈ 0.02) was incubated with EB211 (200 μg/mL), EB279 (200 μg/mL), CS (1 μg/mL), or PBS in the absence or presence of 20 mM MgSO₄ for five hours. At 30 min and five hours of incubation, the mixtures were plated on LB agar, followed by the enumeration of colonies grown after 18 hours of incubation at 37°C. At a high concentration of Mg²⁺, EB211, EB279, and CS were ineffective against *P. aeruginosa* ATCC 27853. The results represent the mean ± standard error of the mean (SEM) of three independent experiments run in triplicate. Statistical significance was determined by one-way analysis of variance (ANOVA) for each time point, followed by Dunnett's multiple-comparison test against the PBS control group.

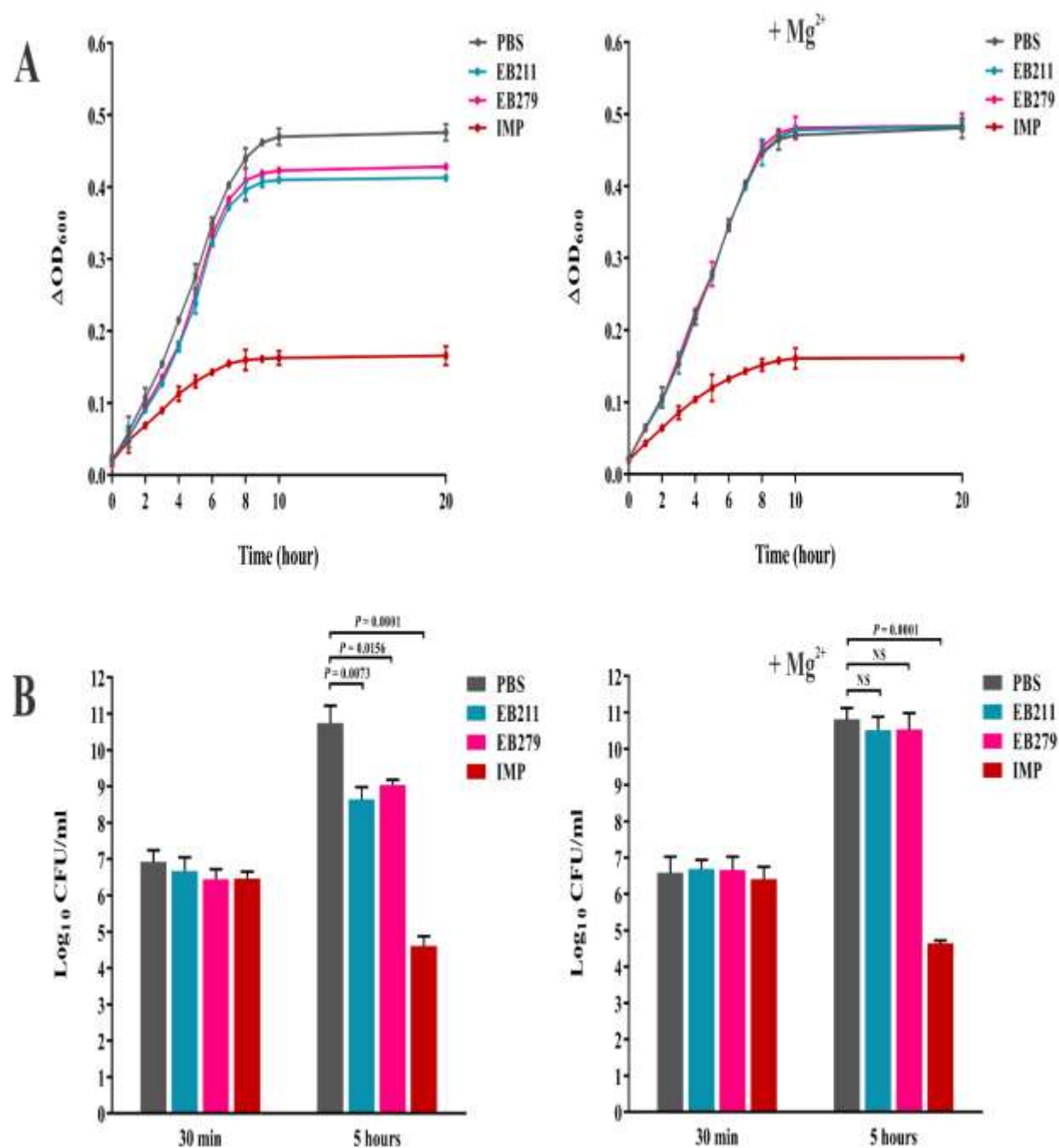


Fig. 5 Antibacterial activity of EB211 and EB279 against *K. pneumoniae* ATCC 700603 was nullified in the presence of a high concentration of Mg²⁺. **(A)** Microtiter plate assay. *K. pneumoniae* ATCC 700603 (OD₆₀₀ ≈ 0.02) was incubated with EB211 (200 μg/mL), EB279 (200 μg/mL), imipenem (IMP) (0.125 μg/mL), or phosphate-buffered saline (PBS) in the absence or presence of 20 mM MgSO₄ for 20 hours. The growth was monitored by reading the optical density at 600 nm every hour for 10 hours and after 20 hours. The effect of EB211 and EB279 on the growth curve of *K. pneumoniae* ATCC 700603 disappeared in the presence of 20 mM MgSO₄, while IMP sustained its growth inhibitory effect. **(B)** Agar plate assay. *K. pneumoniae* ATCC 700603 (OD₆₀₀ ≈ 0.02) was incubated with EB211 (200 μg/mL), EB279 (200 μg/mL), IMP (0.125 μg/mL), or PBS in the absence or presence of 20 mM MgSO₄ for five hours. At 30 min and five hours of incubation, the mixtures were plated on LB agar, followed by the enumeration of colonies grown after 18 hours of incubation at 37°C. At a high concentration of Mg²⁺, EB211 and EB279 were ineffective against *K. pneumoniae* ATCC 700603. In contrast, IMP was effective against *K. pneumoniae* ATCC 700603. The results represent the mean ± standard error of the mean (SEM) of three independent experiments run in triplicate. Statistical significance was determined by one-way analysis of variance (ANOVA) for each time point, followed by Dunnett's multiple-comparison test against the PBS control group.

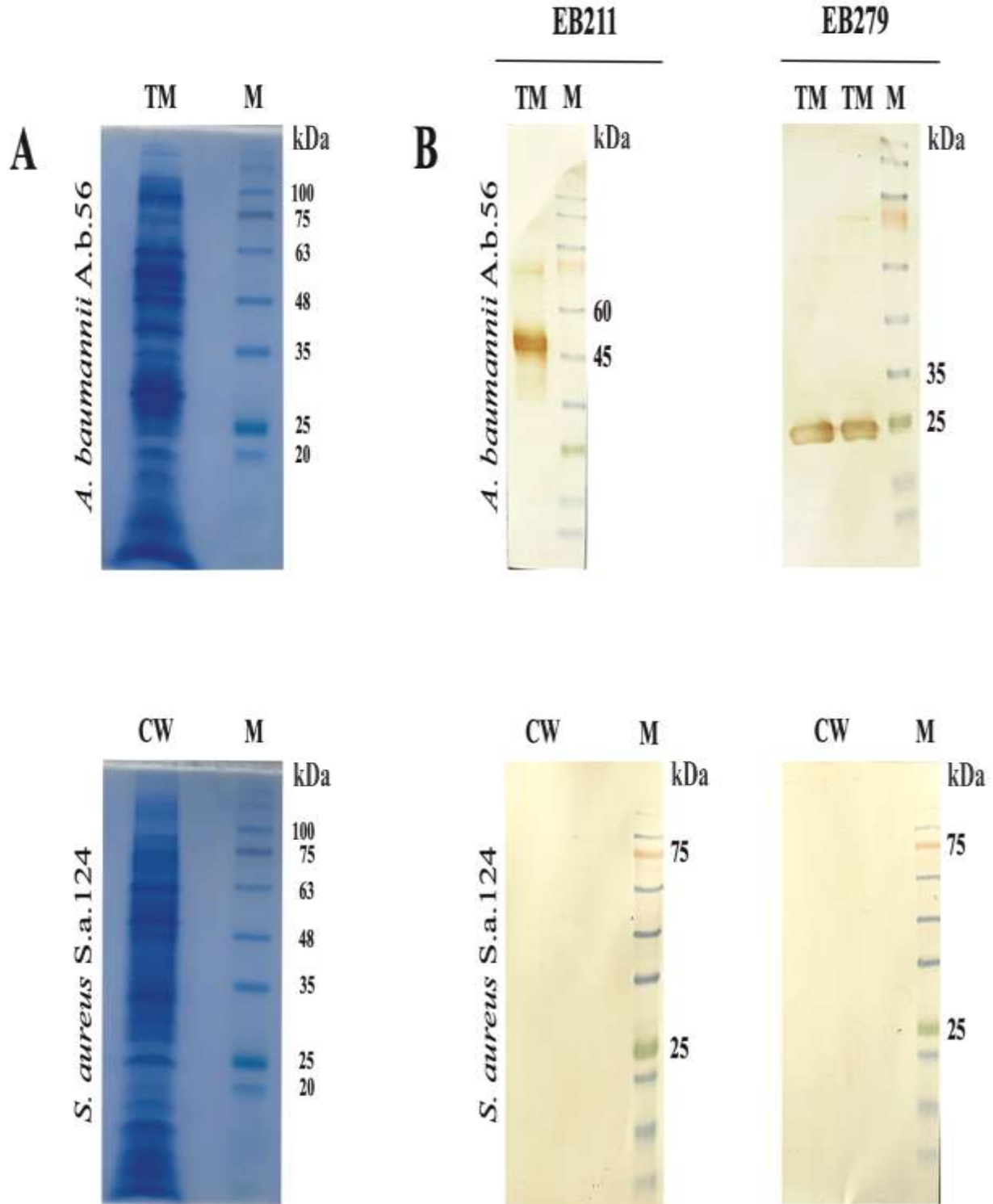


Fig. 6 EB211 and EB279 interacted with membrane proteins of *A. baumannii* but not with cell wall proteins of *S. aureus*. (A) SDS-PAGE. The total membrane extract (TM) of *A. baumannii* A.b.56 and the cell wall extract (CW) of MRSA S.a.124 were run on a 12% SDS-PAGE gel. (B) Immunoblotting. The proteins electrophoretically transferred from an SDS-PAGE gel to the PVDF membranes were incubated with EB211 or EB279, followed by mouse anti-human scFv polyclonal antibody and goat anti-mouse IgG-horseradish peroxidase (HRP)-conjugated antibody. Lane M: protein molecular weight marker.

DISCUSSION

The outer membrane of Gram-negative bacteria is a semi-permeable barrier that makes it difficult for some therapeutic agents to penetrate [26]. In our previous studies, we found two scFvs, EB211 and EB279, demonstrating growth inhibitory activity against *A. baumannii* [1, 18]. Interrupting the integrity of the cell wall and binding to vital macromolecules are the two most imperative mechanisms taken by antimicrobial scFvs to inhibit the growth of bacteria [4, 15, 27]. To find the mechanism of inhibitory activity of EB211 and EB279, three *A. baumannii* strains (*A. baumannii* ATCC 19606, A.b.56, and A.b.58) were treated with the scFv in the presence of a high concentration of Mg^{+2} [28]. Based on the results, the scFvs and CS lost their antibacterial activity against *A. baumannii* in the presence of Mg^{+2} . It has been demonstrated that the bactericidal activity of cationic AMPs is interrupted in the presence of a high concentration of divalent cations (e.g. Mg^{2+}), competing with AMPs for binding to the LPS layer [5, 29-32]. Smart et al. found that as the concentration of Mg^{2+} increased, all binding sites were occupied by Mg^{2+} , and the binding of AMPs to the LPS was disturbed [5]. The activity of EB211, EB279, and CS was negated entirely at a high concentration of Mg^{2+} . Indeed, Mg^{+2} , at high concentration, enhanced the rigidity of the outer membrane and interfered in the interaction of EB211, EB279, and CS with the lipooligosaccharide (LOS) layer [5, 29-33], leading to the inefficiency of the scFvs and the antibiotic against *A. baumannii*. Therefore, we inferred that anti-*A. baumannii* scFvs (with net positive charges due to the existence of basic residues) disrupted the outer membrane by displacing Mg^{2+} from the LOS, a process similar to that observed by colistin against Gram-negative bacteria [34]. In parallel to this, we found in our previous study that three anti-*S. aureus* scFvs (MEH63, MEH158, and MEH183) lost their activity against *S. aureus* in the presence of high concentrations of Mg^{+2} , whereas vancomycin maintained its bactericidal activity [4]. It should be noted that MEH63, MEH158, and MEH183 were able to recognize certain *S. aureus* proteins, including the TrkH family potassium uptake protein (detected by MEH63), as well as PgeF and Ipl8 (detected by both MEH158 and MEH183) [4]. As a result, we concluded that anti-*S. aureus* scFvs exert their antibacterial effects by disturbing the integrity of the cell wall and interrupting the activity of some *S. aureus* proteins [4]. In this regard, we investigated to identify *A. baumannii* proteins that might be recognized by EB211 and EB279. Epitope mapping indicated that EB211 likely binds to ABC transporters, the efflux RND transporter permease subunit, the type IV pilin protein, the OprD family outer membrane porin, and the mechanosensitive ion channel family protein of *A. baumannii*. Based on the results, EB279 may also bind to certain *A. baumannii* proteins, including the PonA, the MFS permease, the TonB family C-terminal domain protein, the type IV pilus modification protein PilV, and

the RND type efflux pump. Notably, all predicted proteins are critical to the viability of *A. baumannii* as well as its resistance to antibiotics [9, 10, 35-46]. To this end, EB211- and EB279-specific candidate targets were assessed with immunoblotting. The western blot results suggested that EB211 and EB279 interact with the OprD and TonB proteins of *A. baumannii*, respectively. The involvement of OprD in nutrient uptake and its membrane abundance allow *A. baumannii* to bypass the nutritional immunity imposed by the host, resulting in colonization, biofilm formation, and pathogenesis [9, 35, 36, 47, 48]. It was demonstrated by Catel-Ferreira et al. that *A. baumannii* OprD, similar to *P. aeruginosa* OprQ, plays an important role in the capture of Mg^{2+} and Fe^{3+} and that it helps the bacteria survive in Mg^{2+} and Fe^{3+} restricted environments [35]. However, there are contradictory studies about the role of OprD (renamed to outer membrane carboxylate channel AB1; OccAB1) in the viability and antibiotic resistance of *A. baumannii* [9, 35-38, 47-52]. The studies by Catel-Ferreira et al. [35] and Smani and Pachon [49] showed that OprD did not affect the susceptibility of *A. baumannii* to carbapenems. Nevertheless, several studies reported the uptake of imipenem by *A. baumannii* OprD [48, 50] and the low expression of OprD in the MDR and PDR *A. baumannii* strains [36, 38, 51, 52]. The study by Cabral et al. showed that the $\Delta oprD$ -like mutant of *A. baumannii* ATCC 17978 developed looser and smaller aggregates than the parent strain [47]. Furthermore, a novel outer membrane protein of the OprD family was found to contribute directly to the virulence of CRAB isolates (the ST2/KL22 clone) [9]. Their results indicated the lower pathogenicity of the hypervirulent DT-Ab057 $\Delta oprD$ mutant, leading to less mortality in infected mice (mortality 50%) compared to mice infected with the wild-type strain (mortality 90%) at 40 hours after challenge [9]. Therefore, they suggested that if the function of OprD was interrupted by agents such as antibodies, *A. baumannii* virulence might decrease with no unwanted impacts on the host microbiota [9].

The EB279 scFv may bind *A. baumannii* TonB, as indicated by the results. In most Gram-negative bacteria, the TonB-ExbB-ExbD energy transducing system facilitates the trafficking of ferric-siderophore, zinc, nickel, vitamin B12, colicin, bacteriophages (e.g. $\phi 80$ and T1), and carbohydrates (e.g. maltose) from the outer membrane to the inner membrane [10, 39-41, 53-57]. The C-terminal domain of TonB interacts with the TonB-box of the TonB-dependent transporter on the outer membrane [39, 53, 58]. In the study by Torres et al., it was found that the $\Delta tonB$ mutant of uropathogenic *Escherichia coli* (UPEC) strain CFT073 had a lower ability to infect the kidneys of mice with ascending urinary tract infection than the wild-type CFT073 [59]. Of note, Yep et al. identified two small molecules (120304 and 175472) showing no inhibitory effect on the growth of the CFT073 mutant lacking TonB. Both molecules exhibited inhibitory activity against the

mutant complemented with pBAD-TonB [57]. Moreover, 120304 prevented the adsorption of bacteriophages $\phi 80$ to *E. coli* MG1655. They concluded that these molecules inhibited UPEC by targeting TonB [57]. In another study, Zimblet et al. found three distinct TonB proteins (TonB₁, TonB₂, and TonB₃) in *A. baumannii* ATCC 19606^T involved in iron uptake and host-pathogen interaction [60]. In this regard, the EB211 and EB279 scFvs may have marked effects on the survival and pathogenicity of *A. baumannii* in the host by targeting OprD and TonB, respectively. There have been several reports of scFvs with direct antibacterial activity by interfering with the function of macromolecules involved in the survival or pathogenesis of bacteria [15, 17, 20]. LaRocca et al. demonstrated that an scFv, generated from a mouse IgM mAb (CB515) specific to the variable small protein of relapsing fever *Borrelia*, exerted its antibacterial activity in a CDC-independent manner [17]. Indeed, the direct bactericidal activity of the CB515 scFv resided in its variable domains, which by specific binding to the variable small protein of relapsing fever *Borrelia*, caused damage in the outer membrane, followed by bacterial lysis [17]. In the studies by Xie et al. [20] and Richard et al. [15], it was demonstrated that an scFv, generated from a fully human mAb against the O-specific antigen of *P. aeruginosa* O6ad, had direct antibacterial activity against *P. aeruginosa* O6ad without aiding the immune system cells or complement. Together, the data emphasize that EB211 and EB279 inhibited the growth of *A. baumannii* mainly by disrupting the outer membrane, which might be followed by binding to and interfering with the biological activity of some macromolecules present on the membrane of *A. baumannii*, including OprD and TonB. Further analysis is required to confirm the latter.

In addition to *A. baumannii*, two other Gram-negative opportunistic pathogens, including *K. pneumoniae* and *P. aeruginosa*, have attracted worldwide attention because of the life-threatening problems that they cause in the medical and health systems [1]. Our previous study indicated that EB211 and EB279 had partially growth inhibitory effects on *K. pneumoniae* and *P. aeruginosa* but not on *S. aureus* [1]. Therefore, the antibacterial activity of EB211 and EB279 against *K. pneumoniae* and *P. aeruginosa* was assessed in the presence of 20 mM MgSO₄, in which both scFvs lost their antibacterial activity similar to colistin. Indeed, positively charged EB211 and EB279 inhibited the growth of *K. pneumoniae* and *P. aeruginosa* by perturbing the outer membrane. The structural similarity between the cell envelopes of *A. baumannii*, *K. pneumoniae*, and *P. aeruginosa*, but not MRSA, might explain why EB211 and EB279 inhibited their growth.

The EB211 and EB279 scFvs disrupted the outer membrane by displacing Mg⁺², inhibiting Gram-negative bacteria growth in this study. It is important to note that although EB211 displayed stronger growth inhibition

than EB279 in all assays, a cocktail of these two scFvs demonstrated significant antibacterial activity against *A. baumannii* in previous studies. Considering that EB211 and EB279 inhibited the growth of *A. baumannii* *in vitro* and demonstrated therapeutic efficacy in an immunocompromised mouse model of pneumonia, it may be considered to treat patients with *A. baumannii* infections using these fully human scFvs in combination with conventional antibiotics in a positive manner.

ACKNOWLEDGEMENT

We thank the Mycobacteriology and Pulmonary Research Department of the Pasteur Institute of Iran for cooperating. This project was granted by the Pasteur Institute of Iran (grant No. 1537).

CONFLICTS OF INTEREST

The authors declare that there are no conflicts of interests associated with this manuscript.

REFERENCES

- Basardeh E, Piri-Gavgani S, Soltanmohammadi B, Ghanei M, Omrani MD, Soezi M, et al. Anti-*Acinetobacter baumannii* single-chain variable fragments show direct bactericidal activity. *Iran J Basic Med Sci.* 2022; 25 (9): 1141-9.
- Whiteway C, Breine A, Philippe C, Van der Henst C. *Acinetobacter baumannii*. *Trends Microbiol.* 2022; 30 (2): 199-200.
- Gan BH, Gaynord J, Rowe SM, Deingruber T, Spring DR. The multifaceted nature of antimicrobial peptides: Current synthetic chemistry approaches and future directions. *Chem Soc Rev.* 2021; 50 (13): 7820-80.
- Soltanmohammadi B, Piri-Gavgani S, Basardeh E, Ghanei M, Azizi M, Khaksar Z, et al. Bactericidal fully human single-chain fragment variable antibodies protect mice against methicillin-resistant *Staphylococcus aureus* bacteraemia. *Clin Transl Immunology.* 2021; 10 (7): e1302.
- Smart M, Rajagopal A, Liu WK, Ha BY. Opposing effects of cationic antimicrobial peptides and divalent cations on bacterial lipopolysaccharides. *Phys Rev E.* 2017; 96 (4-1): 042405.
- Huang W, Zhang Q, Li W, Chen Y, Shu C, Li Q, et al. Anti-outer membrane vesicle antibodies increase antibiotic sensitivity of pan-drug-resistant *Acinetobacter baumannii*. *Front Microbiol.* 2019;10:1379.
- Shadan A, Pathak A, Ma Y, Pathania R, Singh RP. Deciphering the virulence factors, regulation, and immune response to *Acinetobacter baumannii* infection. *Front Cell Infect Microbiol.* 2023; 13: 1053968.
- Dehbanipour R, Ghalavand Z. *Acinetobacter baumannii*: Pathogenesis, virulence factors, novel therapeutic options and mechanisms of resistance to antimicrobial agents with emphasis on tigecycline. *J Clin Pharm Ther.* 2022; 47 (11): 1875-84.
- Hua M, Liu J, Du P, Liu X, Li M, Wang H, et al. The novel outer membrane protein from OprD/Occ family is associated with hypervirulence of carbapenem resistant *Acinetobacter baumannii* ST2/KL22. *Virulence.* 2021; 12 (1): 1-11.

10. Mortensen BL, Skaar EP. The contribution of nutrient metal acquisition and metabolism to *Acinetobacter baumannii* survival within the host. *Front Cell Infect Microbiol*. 2013; 3: 95.
11. Jahangiri A, Owlia P, Rasooli I, Salimian J, Derakhshanifar E, Aghajani Z, et al. Specific egg yolk immunoglobulin as a promising non-antibiotic biotherapeutic product against *Acinetobacter baumannii* pneumonia infection. *Sci Rep*. 2021; 11 (1): 1914.
12. Nielsen TB, Pantapalangkoor P, Luna BM, Bruhn KW, Yan J, Dekitani K, et al. Monoclonal antibody protects against *Acinetobacter baumannii* infection by enhancing bacterial clearance and evading sepsis. *J Infect Dis*. 2017; 216 (4): 489-501.
13. Russo TA, Beanan JM, Olson R, MacDonald U, Cox AD, St. Michael F, et al. The K1 capsular polysaccharide from *Acinetobacter baumannii* is a potential therapeutic target via passive immunization. *Infect Immun*. 2013; 81 (3): 915-22.
14. Wang-Lin SX, Olson R, Beanan JM, MacDonald U, Russo TA, Balthasar JP. Antibody dependent enhancement of *Acinetobacter baumannii* infection in a mouse pneumonia model. *J Pharmacol Exp Ther*. 2019; 368 (3): 475-89.
15. Richard G, MacKenzie CR, Henry KA, Vinogradov E, Hall JC, Hussack G. Antibody binding to the O-specific antigen of *Pseudomonas aeruginosa* O6 inhibits cell growth. *Antimicrob Agents Chemother*. 2020; 64 (4): e02168-19.
16. Richard G. Investigating the bactericidal mechanism of anti-LPS antibodies against *Pseudomonas aeruginosa* Serotype O6. Ontario, Canada: University of Guelph; 2017.
17. LaRocca TJ, Katona LI, Thanassi DG, Benach JL. Bactericidal action of a complement-independent antibody against relapsing fever *Borrelia* resides in its variable region. *J Immunol*. 2008; 180 (9): 6222-8.
18. Basardeh E, Piri-Gavani S, Moradi HR, Azizi M, Mirzabeigi P, Nazari F, et al. Anti-*Acinetobacter baumannii* single-chain variable fragments provide therapeutic efficacy in an immunocompromised mouse pneumonia model. *BMC Microbiol*. 2024; 24 (1): 55.
19. Ahamadi-Fesharaki R, Fateh A, Vaziri F, Solgi G, Siadat SD, Mahboudi F, et al. Single-chain variable fragment-based bispecific antibodies: Hitting two targets with one sophisticated arrow. *Mol Ther Oncolytics*. 2019; 14: 38-56.
20. Xie X, McLean MD, Hall JC. Antibody-dependent cell-mediated cytotoxicity-and complement-dependent cytotoxicity-independent bactericidal activity of an IgG against *Pseudomonas aeruginosa* O6ad. *J Immunol*. 2010; 184 (7): 3725-33.
21. Irani N, Basardeh E, Samiee F, Fateh A, Shooraj F, Rahimi A, et al. The inhibitory effect of the combination of two new peptides on biofilm formation by *Acinetobacter baumannii*. *Microb Pathog*. 2018; 121: 310-7.
22. Pazhouhandeh M, Samiee F, Boniadi T, Khedmat AF, Vahedi E, Mirdamadi M, et al. Comparative network analysis of patients with non-small cell lung cancer and smokers for representing potential therapeutic targets. *Sci Rep*. 2017; 7 (1): 13812.
23. Pazhouhandeh M, Sahraian MA, Siadat SD, Fateh A, Vaziri F, Tabrizi F, et al. A systems medicine approach reveals disordered immune system and lipid metabolism in multiple sclerosis patients. *Clin Exp Immunol*. 2018; 192 (1): 18-32.
24. Dorsey CW, Tomaras AP, Connerly PL, Tolmasky ME, Crosa JH, Actis LA. The siderophore-mediated iron acquisition systems of *Acinetobacter baumannii* ATCC 19606 and *Vibrio anguillarum* 775 are structurally and functionally related. *Microbiology*. 2004; 150 (11): 3657-67.
25. Yasir M, Dutta D, Willcox MDP. Comparative mode of action of the antimicrobial peptide melimine and its derivative Mel4 against *Pseudomonas aeruginosa*. *Sci Rep*. 2019; 9 (1): 7063.
26. Hancock RE. The bacterial outer membrane as a drug barrier. *Trends Microbiol*. 1997; 5 (1): 37-42.
27. LaRocca TJ, Holthausen DJ, Hsieh C, Renken C, Mannella CA, Benach JL. The bactericidal effect of a complement-independent antibody is osmolytic and specific to *Borrelia*. *Proc Natl Acad Sci U S A*. 2009; 106 (26): 10752-7.
28. Rasul R. Novel antimicrobial biomaterials. *Optometry & Vision Science, Faculty of Science, University of New South Wales*. 2010.
29. Wu G, Ding J, Li H, Li L, Zhao R, Shen Z, et al. Effects of cations and pH on antimicrobial activity of thanatin and s-thanatin against *Escherichia coli* ATCC25922 and *B. subtilis* ATCC 21332. *Curr Microbiol*. 2008; 57 (6): 552-7.
30. Hancock R, Wong P. Compounds which increase the permeability of the *Pseudomonas aeruginosa* outer membrane. *Antimicrob Agents Chemother*. 1984; 26 (1): 48-52.
31. Bellamy W, Takase M, Wakabayashi H, Kawase K, Tomita M. Antibacterial spectrum of lactoferricin B, a potent bactericidal peptide derived from the N-terminal region of bovine lactoferrin. *J Appl Bacteriol*. 1992; 73 (6): 472-9.
32. Wang Y, Wang L, Yang H, Xiao H, Farooq A, Liu Z, et al. The spider venom peptide lycosin-II has potent antimicrobial activity against clinically isolated bacteria. *Toxins*. 2016; 8 (5): 119.
33. Zhu X, Dong N, Wang Z, Ma Z, Zhang L, Ma Q, et al. Design of imperfectly amphipathic α -helical antimicrobial peptides with enhanced cell selectivity. *Acta Biomater*. 2014; 10 (1): 244-57.
34. Dubashynskaya NV, Skorik YA. Polymyxin delivery systems: recent advances and challenges. *Pharmaceuticals (Basel)*. 2020; 13 (5): 83.
35. Catel-Ferreira M, Nehme R, Molle V, Aranda J, Bouffartigues E, Chevalier S, et al. Deciphering the function of the outer membrane protein OprD homologue of *Acinetobacter baumannii*. *Antimicrob Agents Chemother*. 2012; 56 (7): 3826-32.
36. Uppalapati SR, Sett A, Pathania R. The outer membrane proteins OmpA, CarO, and OprD of *Acinetobacter baumannii* confer a two-pronged defense in facilitating its success as a potent human pathogen. *Front Microbiol*. 2020; 11: 589234.
37. Kyriakidis I, Vasileiou E, Pana ZD, Tragiannidis A. *Acinetobacter baumannii* antibiotic resistance mechanisms. *Pathogens*. 2021; 10 (3): 373.
38. Rodrigues-Costa F, Cayo R, Matos AP, Girardello R, Martins W, Carrara-Marroni FE, et al. Temporal evolution of *Acinetobacter baumannii* ST107 clone: conversion of bla_{OXA-143} into bla_{OXA-231} coupled with mobilization of ISAba1 upstream occAB1. *Res Microbiol*. 2019; 170 (1): 53-9.
39. Wang J, Xiong K, Pan Q, He W, Cong Y. Application of TonB-dependent transporters in vaccine development of gram-

- negative bacteria. *Front Cell Infect Microbiol.* 2020; 10: 589115.
40. Wilson BR, Bogdan AR, Miyazawa M, Hashimoto K, Tsuji Y. Siderophores in iron metabolism: from mechanism to therapy potential. *Trends Mol Med.* 2016; 22 (12): 1077-90.
41. Hood MI, Mortensen BL, Moore JL, Zhang Y, Kehl-Fie TE, Sugitani N, et al. Identification of an *Acinetobacter baumannii* zinc acquisition system that facilitates resistance to calprotectin-mediated zinc sequestration. *PLoS Pathogens.* 2012; 8 (12): e1003068.
42. Tanaka KJ, Song S, Mason K, Pinkett HW. Selective substrate uptake: the role of ATP-binding cassette (ABC) importers in pathogenesis. *Biochim Biophys Acta Biomembr.* 2018; 1860 (4): 868-77.
43. Booth IR, Blount P. The MscS and MscL families of mechanosensitive channels act as microbial emergency release valves. *J Bacteriol.* 2012; 194 (18): 4802-9.
44. Fernández L, Hancock RE. Adaptive and mutational resistance: role of porins and efflux pumps in drug resistance. *Clin Microbiol Rev.* 2012; 25 (4): 661-81.
45. Piepenbrink KH, Lillehoj E, Harding CM, Labonte JW, Zuo X, Rapp CA, et al. Structural diversity in the type IV pili of multidrug-resistant *Acinetobacter*. *J Biol Chem.* 2016; 291 (44): 22924-35.
46. Fernando DM, Kumar A. Resistance-nodulation-division multidrug efflux pumps in gram-negative bacteria: role in virulence. *Antibiotics (Basel).* 2013; 2 (1): 163-81.
47. Cabral MP, Soares NC, Aranda J, Parreira JR, Rumbo C, Poza M, et al. Proteomic and functional analyses reveal a unique lifestyle for *Acinetobacter baumannii* biofilms and a key role for histidine metabolism. *J Proteome Res.* 2011; 10 (8): 3399-417.
48. Zahn M, Bhamidimarri SP, Baslé A, Winterhalter M, Van den Berg B. Structural insights into outer membrane permeability of *Acinetobacter baumannii*. *Structure.* 2016; 24 (2): 221-31.
49. Smani Y, Pachon J. Loss of the OprD homologue protein in *Acinetobacter baumannii*: impact on carbapenem susceptibility. *Antimicrob Agents Chemother.* 2013; 57 (1): 677.
50. Dupont M, Pages JM, Lafitte D, Siroy A, Bollet C. Identification of an OprD homologue in *Acinetobacter baumannii*. *J Proteome Res.* 2005; 4 (6): 2386-90.
51. Fernandez-Cuenca F, Smani Y, Gomez-Sanchez MC, Docobo-Perez F, Caballero-Moyano FJ, Dominguez-Herrera J, et al. Attenuated virulence of a slow-growing pandrug-resistant *Acinetobacter baumannii* is associated with decreased expression of genes encoding the porins CarO and OprD-like. *Int J Antimicrob Agents.* 2011; 38 (6): 548-9.
52. Asai S, Umezawa K, Iwashita H, Ohshima T, Ohashi M, Sasaki M, et al. An outbreak of *bla*_{OXA-51-like}- and *bla*_{OXA-66}-positive *Acinetobacter baumannii* ST208 in the emergency intensive care unit. *J Med Microbiol.* 2014; 63 (Pt 11): 1517-23.
53. Kim YC, Tarr AW, Penfold CN. Colicin import into *E. coli* cells: a model system for insights into the import mechanisms of bacteriocins. *Biochim Biophys Acta.* 2014; 1843 (8): 1717-31.
54. Killmann H, Videnov G, Jung G, Schwarz H, Braun V. Identification of receptor binding sites by competitive peptide mapping: phages T1, T5, and phi 80 and colicin M bind to the gating loop of FhuA. *J Bacteriol.* 1995; 177 (3): 694-8.
55. Neugebauer H, Herrmann C, Kammer W, Schwarz G, Nordheim A, Braun V. ExbBD-dependent transport of maltodextrins through the novel MalA protein across the outer membrane of *Caulobacter crescentus*. *J Bacteriol.* 2005; 187 (24): 8300-11.
56. Schauer K, Gouget B, Carriere M, Labigne A, de Reuse H. Novel nickel transport mechanism across the bacterial outer membrane energized by the TonB/ExbB/ExbD machinery. *Mol Microbiol.* 2007; 63 (4): 1054-68.
57. Yep A, McQuade T, Kirchhoff P, Larsen M, Mobley HL. Inhibitors of TonB function identified by a high-throughput screen for inhibitors of iron acquisition in uropathogenic *Escherichia coli* CFT073. *mBio.* 2014; 5 (2): e01089-13.
58. Chu BC, Peacock RS, Vogel HJ. Bioinformatic analysis of the TonB protein family. *BioMetals.* 2007; 20 (3-4): 467-83.
59. Torres AG, Redford P, Welch RA, Payne SM. TonB-dependent systems of uropathogenic *Escherichia coli*: aerobactin and heme transport and TonB are required for virulence in the mouse. *Infect Immun.* 2001; 69 (10): 6179-85.
60. Zimble DL, Arivett BA, Beckett AC, Menke SM, Actis LA. Functional features of TonB energy transduction systems of *Acinetobacter baumannii*. *Infect Immun.* 2013; 81 (9): 3382-94.

Cite this article:

Basardeh E, Nazari F, Fateh A, Siadat SD, Oghalaie A, Azizi M, Rahimi-Jamnani F. Two novel single-chain variable fragments, EB211 and EB279, exert antibacterial activity against *Acinetobacter baumannii* by destabilizing the outer membrane. *J Med Microbiol Infect Dis.* 2024; 12 (4): 299-311. DOI: 10.61186/JoMMID.12.4.299.